Solar Phys
DOI 10.1007/s11207-007-0196-8

An Attempt to Detect Coronal Mass Ejections in Lyman-α Using SOHO Swan

M.L. Mays · O.C. St. Cyr · E. Quémerais · S. Ferron · J.-L. Bertaux · S. Yashiro · R. Howard

Received: 3 April 2006 / Accepted: 14 January 2007

Abstract In this study, the possibility that coronal mass ejections (CMEs) may be observed in neutral Lyman-α emission was investigated. An observing campaign was initiated for SWAN (Solar Wind ANisotropies), a Lyman-α scanning photometer on board the Solar and Heliospheric Observatory (SOHO) dedicated to monitoring the latitude distribution of the solar wind from its imprints on the interstellar sky background. This was part of SOHO Joint Observing Program (JOP) 159 and was an exploratory investigation as it was not known how, or even if, CMEs interact with the solar wind and interstellar neutral hydrogen at this distance (≈60 and 120 R_S). The study addresses the lack of methods for tracking CMEs beyond the field-of-view of current coronagraphs (30 R_S). In our first method we used LASCO, white-light coronagraphs on SOHO, and EIT, an extreme ultraviolet imaging telescope also on SOHO, to identify CME candidates which, subject to certain criteria, should have been observable in SWAN. The criteria included SWAN observation time and location, CME position angle, and extrapolated speed. None of the CME candidates that we discuss were identified in the SWAN data. For our second method we analyzed all of the SWAN data for 184 runs of the observing campaign, and this has yielded one candidate CME detection. The candidate CME appears as a dimming of the background Lyman-α intensity represent-

M.L. Mays (✉)
Department of Physics, University of Texas at Austin, 1 University Station C1600, Austin, TX 78712, USA
e-mail: lmays@physics.utexas.edu

O.C. St. Cyr
Laboratory for Astronomy and Solar Physics, NASA Goddard Space Flight Center, Greenbelt, MD 20771, USA

E. Quémerais · S. Ferron · J.-L. Bertaux
Service d'Aeronomie, BP 3, 91371, Verrieres-le-Buisson, France

O.C. St. Cyr · S. Yashiro
Catholic University of America, Washington, DC 20064, USA

R. Howard
Naval Research Laboratory, Washington, DC 20375, USA

ing ≈10% of the original intensity, moving radially away from the Sun. Multiple candidate CMEs observed by LASCO and EIT were found which may have caused this dimming. Here we discuss the campaign, data analysis technique and statistics, and the results.

1. Introduction

Coronal mass ejections (CMEs) are ejections of hot plasma, as well as the magnetic field frozen into that plasma, from large regions of the solar corona; they have typical masses of $10^{14} - 10^{16}$ g of plasma and speeds from 10 to 3000 km s^{-1} with typical average speeds of 400 km s^{-1} (2 R_S h^{-1}) (Hundhausen, 1999; St. Cyr, 2000; Vourlidas *et al.*, 2002). They can be observed in the visible light spectrum with coronagraphs, currently up to 30 R_S with LASCO, and recently with SMEI (a white-light photometer) from 130 R_S to the Earth (Eyles, 2003). Plasma, particle and magnetic properties of CMEs can be measured in situ and detected remotely in the X-ray, EUV, Hα, and radio parts of the spectrum.

Prior to SMEI, the only method of tracking solar disturbances after they depart the coronagraph field-of-view was through low frequency radio observations (Bougeret *et al.*, 1995). However, the WAVES observations track the interplanetary shock which is believed to precede the CME. The Solar Mass Ejection Imager (SMEI) was launched into a sun-synchronous polar orbit on 6 January 2003 on the Coriolis spacecraft. SMEI is sensitive over the optical waveband using CCD cameras. The first clear observations of an interplanetary disturbance tracked by SMEI using the interplanetary scintillation (IPS) method were related to two CMEs detected by LASCO on 28 May 2003 (Tappin *et al.*, 2004). Recent analysis of SMEI data for the 28 October 2003 CME using 3-D solar wind reconstruction techniques allows for visualization of heliospheric structures and their evolution (Jackson *et al.*, 2006).

IPS data sets are synthesized (when available) from ground-based sites and provide information about the line-of-sight electron density and fluctuations. In contrast, the SWAN sensors detect protons, so any distinctions between the behavior of electrons compared to protons might be evident in a comparison. The SOHO observatory is available continuously without a day-night cycle, so if the CME observing campaign had produced a positive detection, then the daily vagaries arising from ground-based observers can potentially be eliminated.

Regardless of their speed at the Sun, interplanetary CMEs are recorded at Earth to be moving at least as fast as the minimum solar wind speed (Lindsay *et al.*, 1999). However, many CMEs are seen to be traveling with speeds greater than the solar wind speed through the LASCO field-of-view, which implies the deceleration of initially fast CMEs outside of the LASCO field-of-view (St. Cyr, 2000). If CMEs can be observed in Lyman-α emission outside of the coronagraph field, SWAN (Solar Wind ANisotropies) would provide this intermediate field-of-view and could potentially offer new insights into CMEs through this novel spectral window.

It is not clear how CMEs interact with the interstellar neutral hydrogen. To investigate this, an observing campaign was begun for the SWAN instrument on board SOHO in May 2002. SWAN is primarily devoted to measuring the large scale structures of the solar wind by observing the distribution of heliospheric neutral hydrogen (Bertaux *et al.*, 1995). The distribution of interstellar H atoms in the solar system is determined by their destruction during ionization charge-exchange with solar wind protons. By moving its two sensors across the sky over three days the instrument produces on average three full-sky Lyman-α (rest

wavelength 121.6 nm) emission maps per week with a resolution of 1°. In normal operation mode SWAN never observes one portion of the sky for long enough to possibly detect a CME, so a new observing campaign was defined and initiated in May 2002. During the campaign the SWAN sensors were held stationary to observe one portion of the sky near the Sun for about fifteen hours a few times each week.

We have analyzed the observations in two ways. First, we searched the LASCO data for CMEs whose extrapolated motions should have placed them in the SWAN field-of-view during a campaign run. Second, we examined all of the campaign observations for signatures of a CME (either an enhancement or a diminishing of Lyman-α intensity) crossing the SWAN field-of-view. Below, we briefly describe the instruments used in the campaign, followed by the observations and results.

2. Description of Instruments

The Solar and Heliospheric Observatory (SOHO) spacecraft orbits around the L1 Lagrange point at 1.5×10^6 km sun-ward from Earth with twelve instruments (Domingo, Fleck, and Poland, 1995). It is a collaborative effort between ESA and NASA. Three instruments, LASCO, EIT, and SWAN, on board this spacecraft were used in this investigation.

2.1. LASCO

The Large Angle Spectroscopic Coronagraph (LASCO) comprises two externally occulted white-light coronagraphs, C2 and C3, as well as a Fe XIV internally-occulted coronagraph, on board SOHO. Together the white-light coronagraphs image the solar corona in visible light from 1.5 to 30 R_S: C2 from 1.5 to 6 R_S and C3 from 3.7 to 30 R_S (Brueckner *et al.*, 1995).

White-light coronagraphs detect photospheric light which has been Thomson-scattered off free electrons in the corona. The radiation recorded at a point in a coronagraph image is a line-of-sight integral of the light scattered along the entire path extending through the corona to the observer or instrument. The ejections of magnetic field and plasma through the corona are detected in a series of coronagraph images as the dynamic phenomena known as CMEs. The true three-dimensional CME electron density structure is projected onto a two-dimensional image (Hundhausen, 1999).

2.2. EIT

The Extreme-ultraviolet Imaging Telescope (EIT) provides wide-field images of the corona and transition region on the solar disk and up to 1.5 R_S above the solar limb. Its normal-incidence multilayer-coated optics can select spectral emission lines from Fe IX (171 Å), Fe XII (195 Å), Fe XV (284 Å) and He II (304 Å) which provide a temperature sensitivity range of 6×10^4 K to 3×10^6 K. The telescope has a 45×45 arcmin field-of-view and 2.6 arcsec pixels to provide a 5-arcsec spatial resolution.

In this study the Fe XII (195 Å) data was used, imaging the corona and transition region boundary and structures inside coronal holes. This corresponds to a peak temperature of $\approx 1.6 \times 10^6$ K. EIT data were used to determine the activity (*i.e.* solar flares and prominence eruptions) and location associated with the appearance of CME candidates potentially detectable with SWAN.

2.3. SWAN

The SWAN instrument on board SOHO is devoted to the measurement of large scale structures of the solar wind using the interstellar neutral hydrogen Lyman-α method. The

30 km s^{-1} flow of uniform interstellar neutral H atoms relative to the Sun is carved by the solar wind because of the charge exchange of solar wind protons with the neutral H atoms. Only those neutral H atoms which have survived ionization may be observed through their resonance scattering of solar photons. SWAN monitors the latitude distribution of the solar wind by mapping the sky in the Lyman-α emission resulting from the scattering (Bertaux *et al.*, 1995).

SWAN is made of a pair of Lyman-α scanning photometers, each with an instantaneous field-of-view of $5 \times 5°$ ($20\ R_S \times 20\ R_S$) with 25 pixels $1 \times 1°$ each. The instrument consists of two gimbaled sensors (SU-Z and SU+Z). Each sensor has an overall field-of-view of over 2π steradians covering the northern and southern ecliptic hemisphere respectively. Because time has to be shared with other kinds of observations, SWAN produces a complete sky map every three days on average (Bertaux *et al.*, 1997). Figure 1 is an example of a typical SWAN sky map in ecliptic coordinates.

SWAN has also detected comets of visual magnitudes between 7 and 11 by detecting the scattering of solar Lyman-α light from neutral hydrogen resulting from the photodissociation of H_2O, the major volatile component of cometary nuclei. However, because SWAN was not

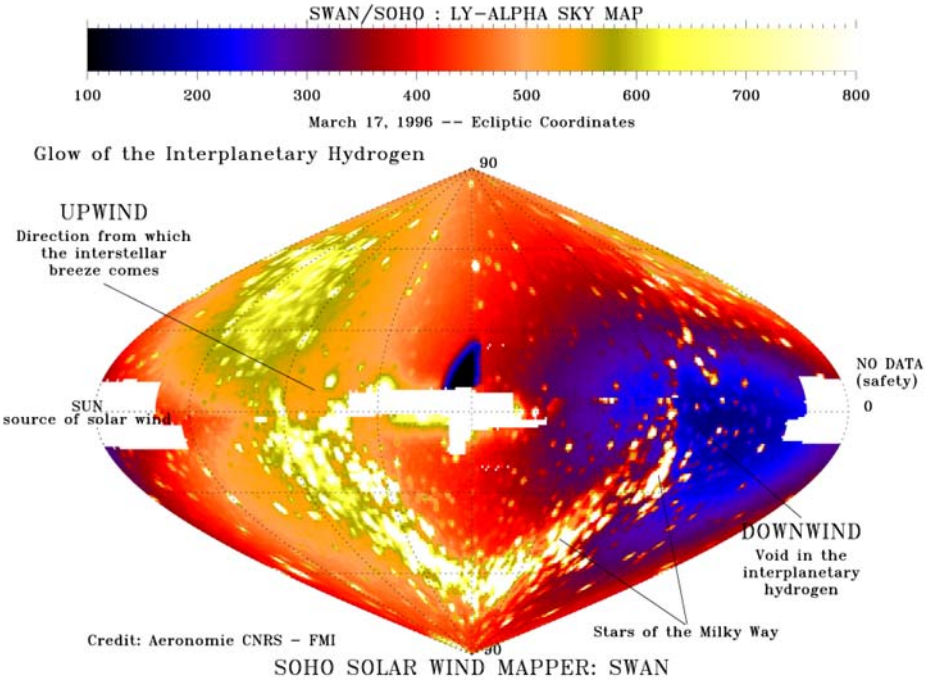

Figure 1 SWAN Lyman-α whole sky map in ecliptic coordinates. The area around the Sun and the anti-solar direction were not covered for safety reasons. The color represents intensity, in counts per second per pixel (one square degree), corresponding to increments of 1.3 Rayleigh. A number of UV hot stars can be identified, tracing the galactic plane. The rest of the ubiquitous emission is due to solar UV Lyman-α photons, backscattered by hydrogen atoms in the solar system. These H atoms are coming from interstellar space, and are approaching the Sun within about 2 AU, in the direction of the incoming flow (ecliptic coordinates; longitude 254°, latitude 7°). A maximum of Lyman-α intensity surrounds this upwind direction. In the opposite direction, the emission is weaker by a factor of 3.5, because most atoms have been destroyed by charge exchange with solar wind protons, creating a cavity void of neutral hydrogen atoms in the downwind direction. A detailed comparison of such Lyman-α maps allows the solar wind mass flux to be determined at all ecliptic latitudes (Bertaux *et al.*, 1997).

designed primarily to detect comets, instrument performance is not ideal. The point spread function of the instrument has a standard deviation comparable to the pixel size near the Lyman-α line, but grows significantly towards the limits of the observing windows of 115 – 170 nm. It also has a slight dependence on observing geometry (Mäkinen *et al.*, 2001). LASCO also detects sungrazing and interloping comets on a regular basis (Biesecker *et al.*, 2002).

3. SWAN Observing Campaign

In normal mode of operation SWAN is unlikely to detect CMEs because the production of full sky maps involves scanning its two sensors across the sky. The SWAN CME observing campaign began in May 2002 so that the instrument could be held stationary with respect to the Sun and potentially detect CMEs. During the campaign, both sensors were held stationary for about 15 hours, positioned on either the east or west limb of the Sun, three or four times a week. The sensors were positioned as close to the Sun as possible, typically with sensor SU-Z at an average distance of 60 R_S and sensor SU+Z at 120 R_S. These distances were selected as the best compromise between closeness to the Sun (to limit the extrapolation of CME motion from LASCO into the SWAN field) and the minimization of stray light from the Sun. Figure 2 shows the LASCO C3 and SWAN configurations for the observing campaign.

The Sun is moving across the celestial sphere at $\approx$30 km s^{-1} and as a result SOHO SWAN, which sees a fixed Sun during this observing campaign, will see the Lyman-α emission from hot UV objects moving across the celestial sphere at $\approx$30 km s^{-1} in the opposite direction. For the nominal orientation of SOHO, the motion of the celestial sphere will be from east to west for SWAN and LASCO. In contrast, all CME motion will be directed radially away from the Sun, therefore the west limb the CME motion coincides with the celestial sphere motion while on the east limb it is opposite. Figure 2 illustrates these motions for the two possible sensor configurations (east and west limb) of LASCO C3 and SWAN SU-Z and SU+Z with arrows indicating the two motions. If SWAN was to detect Lyman-α emission or absorption from CMEs it would see them moving radially away from the Sun, whereas UV stars will only be seen moving from east to west across the field-of-view. For this reason, SWAN observing periods of the east limb where these two motions are opposite is preferable. This guarantees that any motion detected by SWAN that is moving radially away from the Sun must be coming from the Sun and not from the background celestial sphere.

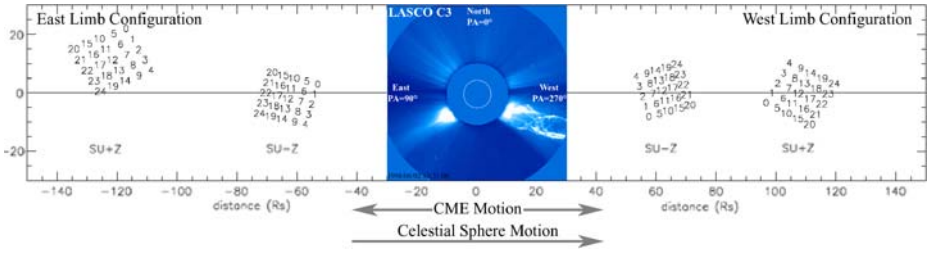

Figure 2 LASCO C3 (3.7 to 30 R_S) and SWAN SU-Z and SU+Z (20 R_S × 20 R_S) sensor configurations for the east and west limbs during the observing campaign. The location of each SWAN sensor pixel is denoted by the pixel number. The directions of celestial sphere and CME motion are indicated.

Table 1 Properties of the four candidate CMEs from LASCO selected based on the criteria outlined in Section 4 and the corresponding SWAN observations. Candidates were selected from 1 822 LASCO CMEs occurring during the first 14 months of the campaign (May 2002 – July 2003). The CMEs were not visible either as an enhancement or as a diminution of intensity in the SWAN data.

Date	Time (UT)	Central PA (degrees)	Width (degrees)	Speed ($km\,s^{-1}$)	SWAN SU+Z and SU-Z observations
2002 May 3	23:18	119	99	902	Celestial sphere motion
2002 May 17	01:50	75	73	800	Celestial sphere motion
2002 Jun 7	17:54	60	69	646	Celestial sphere motion
2002 Aug 22	18:26	108	126	750	Celestial sphere motion

4. Method One: Starting with LASCO CMEs

We have examined all SWAN data acquired through this observing campaign. However, our first approach was to concentrate on CMEs that had been detected by EIT and LASCO and whose extrapolated speeds placed them in the SWAN field-of-view during the observing campaign. Here we describe that method, although no candidate CMEs were identified in SWAN.

Coronal mass ejection candidates selected for this investigation were taken from the SOHO LASCO CME catalog (Yashiro *et al.*, 2004).[1] The selection was based on SWAN observing time and location and CME position angle, width, apparent speed measured in the direction of the SWAN sensors, and EIT observations which placed the associated activity near the sky plane so as to reduce the uncertainty in the extrapolated motion of the CME.

Coronal mass ejections occurring up to 30 hours before the beginning of each SWAN observation period were considered. This duration was based on the fact that a CME traveling at 2 $R_S\,h^{-1}$ ($400\,km\,s^{-1}$, near the average speed for CMEs) reaches the SWAN SU-Z sensor (at $\approx 60\ R_S$) in about 30 hours. CMEs with position angle (PA) and width combinations that did not fall near the angles subtended by the SWAN SU-Z sensor were not considered. Height-time data for the remaining CMEs were extrapolated for intersection with SWAN observing times and sensor location. The accuracy of the speed measurements from the height-time data was evaluated by examining EIT images for other solar activity located near the solar limb associated with the appearance of the CMEs.

Based on these criteria we selected four excellent CME candidates of the 1 822 LASCO CMEs occurring during the first 14 months of the campaign (May 2002 – July 2003). However, there was no indication that these candidate CMEs were visible either as an enhancement or as a diminution in the corresponding SWAN observations. The properties of these CMEs and SWAN observations are listed in Table 1.

5. Method Two: Starting with SWAN Observations

All of the 184 SWAN observing runs for the first two years of the campaign (May 2002 – 2004) were examined for the presence of candidate CMEs. The results could be divided into five categories: bad data, constant or only celestial sphere motion, large scale darkening or

[1] http://cdaw.gsfc.nasa.gov/CME_list/.

Table 2 Categorized results from the analysis of SWAN intensity plots and movies for each of the 184 observation runs for each sensor (see Section 5). This table shows how many observation runs fell into each category. The runs are further divided to show how many runs in each category where in which sensor and which limb was being observed.

	All	SU+Z	SU-Z	East	West
Bad data	18	8	10	2	16
Constant/celestial sphere motion	286	157	129	69	217
Large scale darkening	41	2	39	8	33
Large scale brightening	22	16	6	6	16
Candidate CMEs	1	1	0	1	0
Total	368	184	184	86	282
Total observing runs	184			43	141

brightening, and candidate CMEs. For large scale brightening, most of the pixels increased in intensity by roughly the same amount over the observing period. Similarly, for a large scale darkening, pixels diminished in intensity during the observation. These both appear to be instrumental effects and have not been interpreted as signatures of CMEs. The constant category includes quiet data with relatively unchanging intensities. Celestial sphere motion describes the observation of bright sources moving on the time scale of the revolution of the celestial sphere. Data with breaks in the observation or other problems were skipped and categorized as "bad data". Table 2 shows the resulting statistics for these examinations and, because of the celestial motion versus CME motion discussed above, we focus on the column labeled east. Of the 184 SWAN observing runs, only one could be categorized as a candidate for a CME observation.

5.1. Pixel-by-Pixel Analysis

For this observing campaign, the SWAN data are time series of Lyman-α intensity (measured in counts/second) for each of the 25 pixels. These intensities were plotted for the observation duration along with a running standard deviation computed for every 100 data points. The integration time for each sample was 28 seconds. A collection of all 25 individual intensity plots was made for the SWAN data as shown in Figure 3 for 24 August 2002. These plots are positioned to correspond to SU+Z pixel locations and the arrow shows the line towards the Sun given the sensor configuration shown in Figure 2.

5.2. Time-Sequence Movie Analysis

A movie tool to examine time sequences of data, similar to those used for LASCO and EIT image analysis, was built for the SWAN data. The pixels in the time-sequence movies are represented as squares and are positioned to correspond to sensor pixel locations. The frames in the movie show the intensity plots in time with a 10-minute time cadence. Four movie frames for 24 August 2002 are shown in Figure 4 and the corresponding intensity plots in Figure 3. The arrow shows the line towards the Sun given the sensor configuration shown in Figure 2. Direct, base difference, and running difference movies were analyzed for all of the campaign runs. Direct movies simply show the pixel intensity mapped to the movie color table. In base difference movies the first frame has been subtracted from all subsequent frames, so if the intensity increases, decreases, or remains the same with time, the pixel becomes respectively brighter, darker, or appears gray. Running difference movies are created by subtracting the previous frame from every frame.

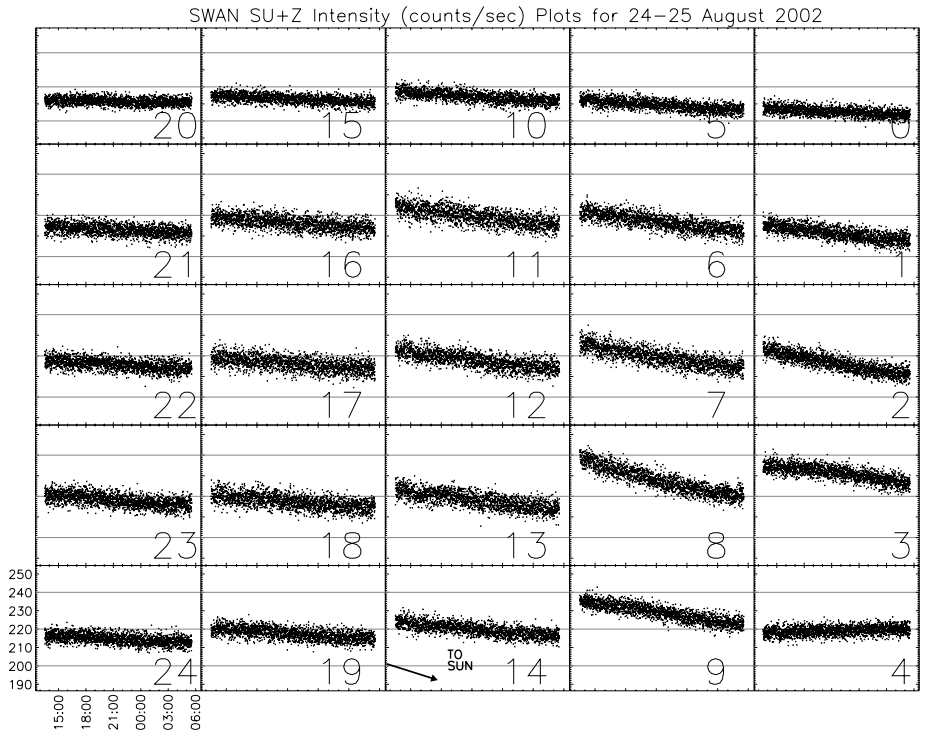

Figure 3 Intensity (counts/s) vs. time plots of 25 SU+Z sensor pixels for SWAN observing period on 24 – 25 August 2002. SWAN SU+Z was located at 122 R_S and 85°. These plots are positioned to correspond to SU+Z pixel locations and the arrow shows the line towards the Sun given the sensor configuration shown in Figure 2.

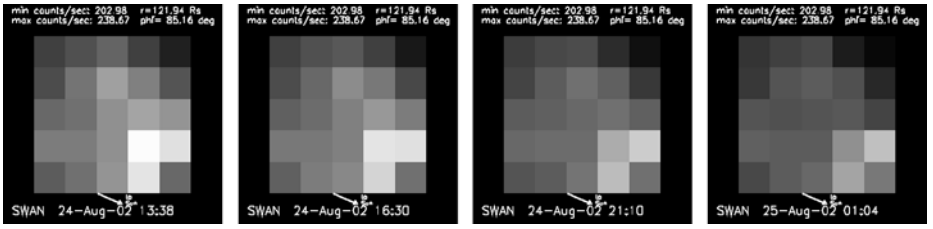

Figure 4 Frames from a time-sequence movie for SU+Z SWAN data for the observation period 24 August 2002 (these correspond to the intensity data shown in Figure 3). The movie has a black and white color table where white corresponds to the highest intensity observed.

6. Observations During 22 – 25 August 2002

6.1. SWAN

On 24 August 2002 the campaign was run off the east limb as shown in the bottom panel Figure 2. Sensor SU+Z was located at 121.94 R_S and 86.16°. The intensity plots shown in Figure 3 and time-sequence movies shown in Figure 4 were analyzed. A closer look at the pixels of interest in the intensity plots is shown in Figure 5. Beginning at about 15:00 UT

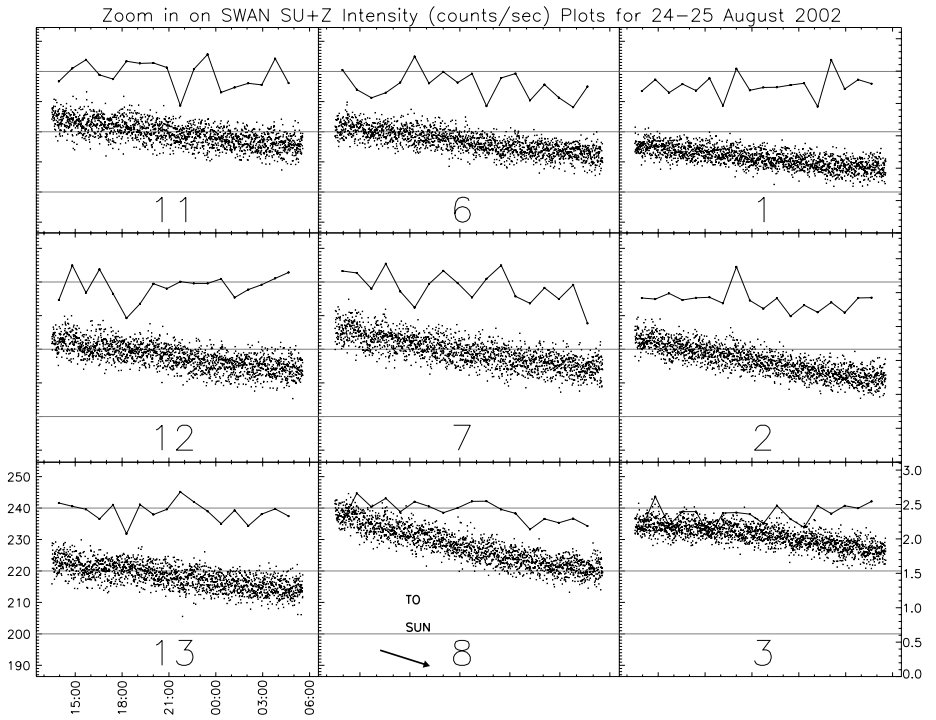

Figure 5 Zoom in on pixels of interest in Figure 3 of the intensity (counts/s) vs. time plots for SWAN observing period 24 – 25 August 2002. The running standard deviation, calculated every 100 points, is plotted against the opposite y-axis and shown as a solid line.

the SWAN pixels 2, 7, 8, and 9 in sensor SU+Z began to diminish in intensity from the base levels at 13:38 UT. The motion of the diminishing intensity was radially away from the Sun. The expansion of the diminishing intensity continued fully into pixels 1, 5, 6, 11, 12, 13, and 14 at about 21:00 UT before the observation ended at 03:48 UT on 25 August Pixel 8 diminished the most and overall this represented a decrease of ≈10% in this pixel. Measurement of the motion of the darkening pixels from the movie is difficult. Crude estimates by several observers suggest that the apparent speed of motion is $\leq$100 km s^{-1}, which is slower than we expect for a CME. If the darkening represents a diminution that is significantly projected onto the sky plane, then the speed could be much larger. Only celestial sphere motion was observed in sensor SU-Z which was located at 92.76 R_S and 63.04°.

6.2. LASCO and EIT

The LASCO and EIT data prior to the 24 August 2002 SWAN observation period was examined, and three candidate CMEs near the Sun were found. The extrapolated height-time plots for the leading edges of each of these events is shown in Figure 6. From this figure it is clear that, given the uncertainties of the speed extrapolations, any of the three (or a combination) could have intersected the SWAN SU+Z sensor during this observing run. Below we describe the LASCO/EIT observations of these CMEs.

On 22 August 2002 a small, amorphous, faint fan appeared in the LASCO field-of-view at position angle ≈90° at 14:50 UT and could be tracked through the C2 field-of-view, head-

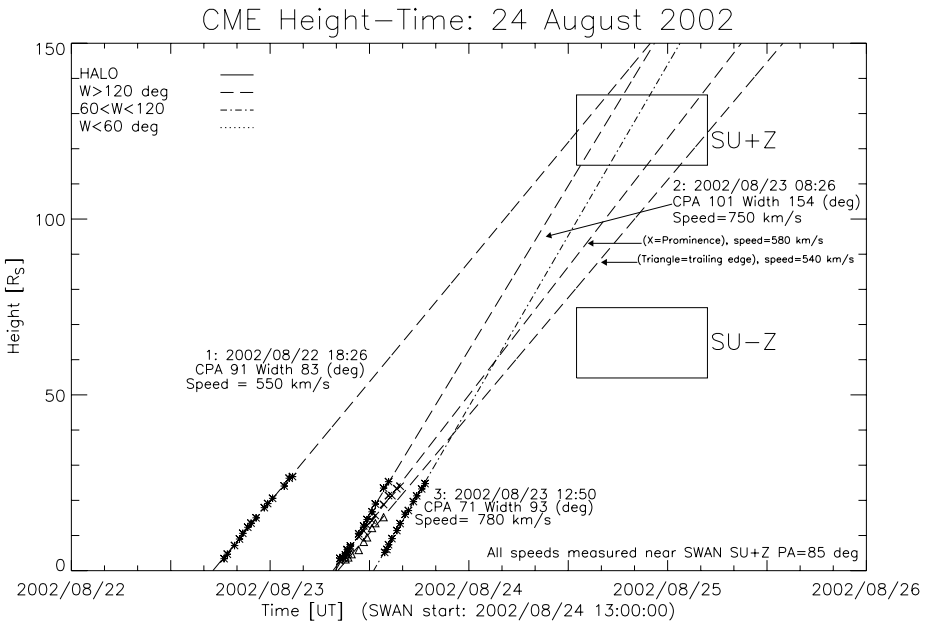

Figure 6 CME extrapolated height-time plot from LASCO data for SWAN observation period 24 August 2002. The three CMEs are denoted by the dashed lines with asterisks. The two other dashed lines are the height-time extrapolation for the prominence and trailing edge of the second CME on 2002/08/23 08:26 UT, denoted by the crosses and triangles respectively. The two boxes represent the radial width of the SU+Z and SU-Z sensors in height and observations duration in time.

ing somewhat southeast. It spanned position angles 77° to 97° and moved with a speed of ≈310 km s^{-1}. The extrapolated speed of this event means that it should miss the SWAN SU+Z field-of-view, but we mention it for completeness. There was no major activity detected in the EIT images that could be associated with this CME.

Before the 22 August 2002 14:50 UT CME had departed the C2 field, it was followed by a second, much brighter CME that appeared at 18:26 UT. This event had a very structured interior that appeared to be a flux rope (Chen *et al.*, 1997), except it was mostly filled (as opposed to being a cavity). The CME spanned position angles 57 to 120°, and it moved with a speed of 550 km s^{-1}. In EIT images, active region NOAA 10087 at S06E76 was seen to erupt at the east limb beginning at 17:24 UT with a bright filament eruption and subsequent coronal dimming above the limb.

The first CME on 23 August 2002 appeared as a faint filled front at position angle ≈80° at 06:26 UT. At 08:26 UT a bright structured prominence appeared in a C2 image at the same location. Figure 7 shows EIT, LASCO C2 and C3 frames for this event. There was a circular structure embedded in the northeast portion of this event. The entire event spanned position angle ≈50 to 135°, and there were faint extensions to the north and south. This CME traveled through the LASCO field-of-view with a speed of 750 km s^{-1}. Flows continued until the next event, described below. In EIT observations, this CME was clearly associated with active region NOAA 10085 located at S12E21. Part of it blew out to the east limb, but the most distinguishable part was a prominence that traveled across the Sun toward the west limb. The part traveling east appeared to trigger a series of events from active region NOAA 10087 near the east limb. For this CME event the prominence and trailing edge measurement

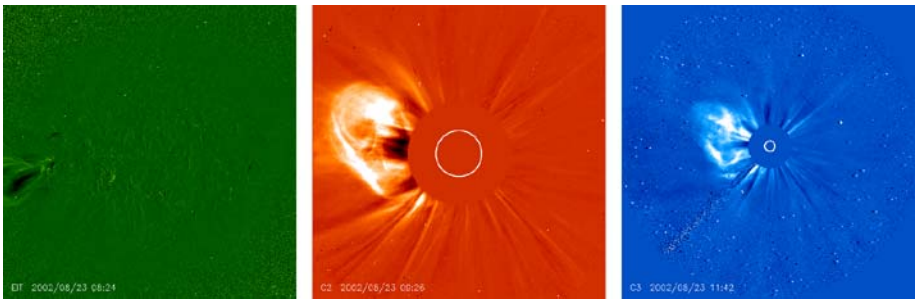

Figure 7 EIT (Fe XII (195 Å), shown on left), LASCO C2 (field-of-view 1.5 to 6 R_S, shown in middle), and LASCO C3 coronagraph (field-of-view 3.7 to 30 R_S, shown on right) for the 23 August 2002 08:26 UT CME. The white circle in the LASCO frames shows the relative size and location of the solar disk.

is included in the height-time plot, in addition to the leading edge measurement shown in Figure 6.

The second candidate CME on this date appeared at 13:50 UT in the northeast and over the north pole and northwest. In northeast it was a faint filled front that was the leading feature for the entire structure. It is not clear if this was a separate overlapping event from the north and northwest, or if it was a single CME. The span was from PA ≈240 to 110°. There may have been some structure in the northeast, and the event was much slower at other PAs. It traveled 780 km s^{-1} in the northeast. Based on EIT data, this event was clearly the result of the earlier CME triggering Active Region #0087 at the east limb, which had grown a loop arcade that flared again at 13:13 UT, associated with this CME.

7. SWAN Observations During 20 May 2004

An east limb SWAN observing run on 20 May 2004 showed observations of a comet in sensor SU+Z located at 124.09 R_S and 83.71°. Pixels in the sensor corner closest to the Sun diminished in intensity in the direction towards the Sun, with a starting intensity of 200 to 400 counts/s, which was well above the background 120 to 150 counts/s. Towards the end of the observation the intensity diminished rapidly representing a decrease of ≈65% in the darkest pixel in ≈3 h. SWAN comet images show 2 or 3 very bright comets close to the Sun during this period of time, so it is likely that the count rates above 200 counts/s are caused by cometary emission. Only celestial sphere motion was observed in sensor SU-Z located at 61.76 R_S and 89.60° with count rates of 50 to 90 counts/s.

8. Discussion

Since the extrapolation of the LASCO CME speeds in the first method did not uncover any candidates in SWAN, it is possible that the extrapolation is not valid. The CMEs could have accelerated or decelerated to miss the SWAN observing window. However, it is highly unlikely that the CMEs would have accelerated as they show constant speeds in the LASCO C3 field-of-view and CME acceleration is uncommon (Hundhausen, 1999; St. Cyr, 2000). It is also unlikely that the CMEs would have decelerated enough to miss the SWAN window entirely.

To test the sensitivity of our analysis to detect CMEs, a simple quantitative model of intensity (counts/s) increases and decreases of SWAN data was made. The simulated data indicated that a 1% increase/decrease in the signal (counts/s) over the period of one hour was not discernible using the visual method described above, based on the actual standard deviations of SWAN data. A 5% increase/decrease was discernable, and a 10% increase/decrease could be readily detected. The period of one hour was chosen because a 2 R_S h^{-1} CME would traverse the distance of ≈ 4 R_S across a SWAN pixel in about 2 h. We conclude that an increase/decrease of intensity of at least 5% is required to detect a CME in these data.

The following possibilities regarding CME detection in Lyman-α by SWAN are discussed:

1. Can SWAN see CMEs in emission? If the CME velocity in the Sun's rest frame is larger than 150 km s^{-1} the neutral hydrogen in the CME will be outside of the solar line. We do not expect a lot of Lyman-α photons from the recombination of protons and electrons. Therefore, we do not expect a brightening in the field-of-view due to the passage of a CME. If there is a brightening it is more likely to come from the Sun.
2. If the CME contains a neutral hydrogen component, this component can behave like a hydrogen absorption cell and absorb a fraction of the interplanetary background, which comes from outside 1 AU. There is no Doppler shift because the line-of-sight and the velocity of the CME atoms are almost perpendicular. However, this method is also improbable because it is likely that all of the neutral hydrogen component contained in the CME will be quickly photo-ionized.
3. Can SWAN see CMEs in absorption? The protons in a high-proton density CME could destroy enough interplanetary hydrogen to cause a signal decrease. However, within 1 AU most of the hydrogen atoms are already ionized and according to SWAN models all of the atoms are already ionized within 0.5 AU. Consequently, even a very large cloud of protons will have nothing left to ionize unless there is an inner source of neutral hydrogen, such as the outgasing of dust.

   A simple Lyman-α optical thickness calculation and extinction estimate can be made as follows. The line center cross section is given by $\sigma = 5.96 \times 10^{-12} T^{-1/2}$ (cm^2) and the line center optical thickness by $\tau = \sigma n_H l$, where n_H is the density of the H atoms and l is the line-of-sight length of the CME. For a temperature of $T = 20\,000$ K and 10% neutral material, the radial variation of the neutral density is estimated to be $1/r^3$ where r is the radial distance from the Sun in units of R_S. The length of the CME along the line-of-sight is $l = l_0(r/215)$ where $l_0 \approx 1$ R_S is the length at 1 AU. The density now becomes $n_H = 5k(215/r)^3(1/10)$, where k is the factor of density increase due to the CME from normal solar wind and $k = 1$ is the mean solar wind density ($n_p = 5$ cm^{-3} for 1 AU). If $k = 10$ is assumed, the density becomes $n_H = 5(215/r)^3$ cm^{-3}, which yields $\tau = 0.18$ for 60 R_S and 0.05 for 120 R_S. However, these numbers are conservative and could be increased by major events to $\tau \approx 0.4$.

   One possible explanation for not seeing absorption events all the time is that the photoionization destroys the neutral H. The photoionization rate at 6.8 R_S is 8×10^{-5} s^{-1} (Raymond *et al.*, 1998). When the gas is within a few R_S, the cloud of neutrals may be thick enough to shield many of the neutrals, as the radiation ionizes the prominence gas. For comparison, the recombination rate is small. In one event seen by SOHO UVCS (Akmal *et al.*, 2001) the density was 10^6 cm^{-3} at 3.5 R_S. This gives a recombination rate of $\approx 4 \times 10^{-6}(1/r^3)$ s^{-1} and a photoionization rate of $\approx 0.004(1/r^2)$ s^{-1}. Therefore, in order to see absorption events a very massive prominence eruption or one fast enough to reach 60 R_S quickly is needed.

9. Summary

SOHO data from SWAN, EIT and LASCO were analyzed to investigate if CMEs could be observed in neutral Lyman-α emission or absorption. This was done to investigate if CMEs interact with the interstellar neutral hydrogen and we hoped this would give a new window for observing CMEs beyond the field-of-view of present day coronagraphs. Our observing campaign ran 184 times between May 2002 – 2004.

In the first method, candidate events chosen based on selection criteria from 1 822 LASCO CMEs occurring during May 2002 – July 2003 were not visible in SWAN observations. From the second method, there was one observational run where a progressive diminishment in SWAN Lyman-α intensity was detected that appeared to move away from the Sun and counter the motion of the celestial sphere. Multiple CMEs were identified in LASCO and EIT images with extrapolated speeds which placed them in the SWAN SU+Z sensor field-of-view. However, the candidate had not been predicted based on the extrapolated LASCO/EIT point-of-view. In retrospect, the candidate CME that may account for the Lyman-α darkenings was identified in LASCO and EIT images, but there were no distinguishing characteristics of these events over the other 9000+ CMEs in the SOHO LASCO CME catalogue that suggested why this SWAN observational run was different from the other 183.

Acknowledgements We wish to acknowledge the contributions and support of Professor Fred Bruhweiler at The Catholic University of America, Professor Glenn Mason at the University of Maryland, Sam Freeland at Lockheed-Martin, J. Keith Feggans, and Linda Greenslade at NASA Goddard Space Flight Center. We would also like to thank John Raymond (Harvard-Smithsonian Center for Astrophysics/SAO) for useful discussions. Much of the work was done through CUA while M.L. Mays was an undergraduate student at the University of Maryland College Park. Seiji Yashiro is supported through NASA grant #NNG05GR03G. The SOHO LASCO CME catalog is generated and maintained by NASA and The Catholic University of America in cooperation with the Naval Research Laboratory. SOHO is a mission of international cooperation between the European Space Agency and NASA.

References

Akmal, A., *et al.*: 2001, *Astrophys. J.* **553**, 922.
Bertaux, J.L., *et al.*: 1995, *Solar Phys.* **162**, 403.
Bertaux, J.L., *et al.*: 1997, *Solar Phys.* **175**, 737.
Biesecker, D.A., Lamy, P., St. Cyr, O.C., Llebaria, A., Howard, R.A.: 2002, *Icarus* **157**, 323.
Bougeret, J.-L., *et al.*: 1995, *Space Sci. Rev.* **71**, 231.
Brueckner, G.E., *et al.*: 1995, *Solar Phys.* **162**, 357.
Chen, J., *et al.*: 1997, *Astrophys. J.* **490**, L191.
Domingo, V., Fleck, B., Poland, A.I.: 1995, *Solar Phys.* **162**, 1.
Eyles, C.J.: 2003, *Solar Phys.* **217**, 319.
Hundhausen, A.J.: 1999, In: Strong, K.T., Saba, J.L., Haisch, B.M., Schmelz, J.T. (eds.) *The Many Faces of the Sun*, Springer, New York, p. 143.
Jackson, B.V., Buffington, A., Hick, P.P., Wang, X., Webb, D.: 2006, *J. Geophys. Res.* **111**, A04S91.
Lindsay, G.M., Luhmann, J.G., Russell, C.T., Gosling, J.T.: 1999, *J. Geophys. Res.* **104**, 12515.
Mäkinen, J.T.T., *et al.*: 2001, *Astron. Astrophys.* **368**, 292.
Raymond, J.C., *et al.*: 1998, *Astrophys. J.* **508**, 410.
St. Cyr, O.C.: 2000, *J. Geophys. Res.* **105**, 8169.
Tappin, S.J., *et al.*: 2004, *Geophys. Res. Lett.* **31**, L02802.
Vourlidas, A., Buzasi, D., Howard, R.A., Esfandiari, E.: 2002, In: Wilson, A. (ed.) *Solar Variability: From Core to Outer Frontiers, ESA SP-506*, 91.
Yashiro, S., *et al.*: 2004, *J. Geophys. Res.* **109**, A07105.